Engineering Structures 191 (2019) 82–91

Contents lists available at ScienceDirect

Engineering Structures

journal homepage: www.elsevier.com/locate/engstruct

Experimental investigation of shear walls using carbon fiber reinforced polymer bars under cyclic lateral loading

Qi Zhao[a], Jun Zhao[b,*], Jun-Tao Dang[a], Ji-Wei Chen[c], Fu-Qiang Shen[a]

[a] College of Civil Engineering, Zhengzhou University, Zhengzhou 450001, China
[b] College of Mechanics and Engineering Science, Zhengzhou University, Zhengzhou 450001, China
[c] Architectural Design and Research Institute of Henan Province Co. LTD, Zhengzhou 450000, China

ARTICLE INFO

Keywords:
Shear wall
CFRP bars
Seismic behavior
Residual deformation
Self-centering behavior
Cyclic loading

ABSTRACT

The aim of this paper was to investigate the seismic behavior of shear walls reinforced with CFRP (carbon fiber reinforced polymer) bars as longitudinal reinforcement. Three full-scale shear walls with same geometry and dimension were tested up to failure under pseudostatic cyclic lateral loading. The first one was a conventional reinforced wall (as a reference specimen). The second was reinforced with steel bars in boundary elements and CFRP bars in the wall web as vertical reinforcements. The third was reinforced with CFRP bars totally in the vertical direction. Residual deformations and cracks were of particular interest. The experimental results show that the CFRP-reinforced shear wall achieved comparable lateral strength, post-yield stiffness, acceptable lateral drift and lower level of energy dissipation compared with the reference wall. Besides, excellent self-centering behavior was observed, and the residual deformation of CFRP-reinforced shear walls decreased by more than 50% compared to the reference wall at a lateral drift of 1.0%. These promising results demonstrate the feasibility of CFRP bars as linear-elastic material to achieve self-centering behavior of shear wall.

1. Introduction

Shear walls are designed to resist lateral forces induced by winds and seismic events. And conventional reinforced concrete shear walls have been proved to be an excellent, cost-effective lateral-resisting system in modern high-rise reinforced concrete buildings during natural disasters [1–8]. Zinov'ev and Smerdov [9] believe that the dynamic behavior of structures, to a great extent, depends on the energy absorption (damping) ability. According to this theory, researchers on traditional reinforced concrete shear walls emphasized the importance of ductility and energy dissipation. By making full use of the excellent plastic deformation performance of steel bars, enough energy could be absorbed during natural disasters to achieve ductile failure and avoid collapse [10–12]. However, the low yield strain of steel bars may result in large residual deformations, and they cannot get back into shape by themselves. As a result, large lateral deformations will remain in buildings after earthquake. Things may get worse when aftershocks happen, then buildings may become unsuitable to maintain their serviceability. Besides, residual displacements will cause considerable costs to repair these damaged buildings. Some of them even have to be demolished due to severe damages [13]. Consequently, controlling residual deformations of structures after earthquakes is crucial for them to maintain sustainability and serviceability [14–16]. With the development of seismic design, self-centering behavior and residual deformation after experiencing large lateral displacements become critical factors. They indicate whether damaged structures could be repaired or buildings can maintain in service.

Fiber reinforced polymer (FRP) materials for construction were initially used to solve the corrosion of steel reinforcement and to repair the damaged structures. Glass fiber-reinforced polymer (GFRP) bars, basalt fiber-reinforced polymer (BFRP) bars and carbon fiber-reinforced polymer (CFRP) bars are several common types of them. They have excellent tensile strength up to more than 1000 MPa and remain elastic until fracture without yielding during the tension test. The main concerns towards FRP bars for construction are their brittle failures and bond-slip conditions when they work together with concrete. Fig. 1 illustrates stress-strain curves of FRP bars in comparison to steel bar. Their expected tensile fractures of FRP bars for use are also marked.

Several pioneers have made an attempt to use FRP bars as flexural reinforcement to mitigate the residual displacements. Mohamed et al. [3,5] evaluated the seismic behavior of three GFRP exclusively reinforced walls under cyclic loading. These walls failed due to concrete crushing and reached their flexural capacity and acceptable lateral drifts. They also exhibited reasonable recoverable behavior before

* Corresponding author.
E-mail address: zhaoj@zzu.edu.cn (J. Zhao).

https://doi.org/10.1016/j.engstruct.2019.04.052
Received 1 August 2018; Received in revised form 14 April 2019; Accepted 17 April 2019
0141-0296/ © 2019 Published by Elsevier Ltd.

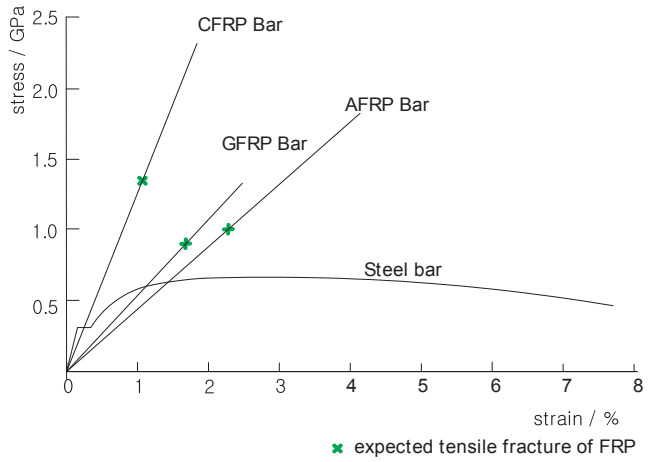

Fig. 1. Stress – strain curves of FRP and steel bars.

moderate damage. Cai and Wang [17] tested six cantilever columns with variable reinforcement ratios of CFRP and steel bars under constant axial loads and reversed lateral loading. Their studies show that the post-yield stiffness was improved and residual displacements decreased dramatically when additional CFRP bars were added into the conventional columns. Besides, the hysteretic energy dissipation of these specimens remained the same as that of the reference. By contrast, the increase of steel-reinforcement contributed little to the post-yield stiffness and self-centering performance. Ghazizadeh and Cru-Noguez [18,19] compared the behavior of a steel fiber-reinforced concrete (SFRC) wall reinforced with FRP-steel bars as flexural reinforcement with a traditional RC wall under cyclic loading. The new specimen achieved goals of self-centering and mitigating residual displacements apart from similar strength, stiffness and ductility as RC shear wall. They also developed a finite-element analysis model for hybrid GFRP-steel reinforced walls for moderate seismic demands which can be used to identify the best hybrid-reinforced scheme.

Fig. 1 also shows that for various FRP materials, the CFRP bars have better tensile strength and closer elastic modulus to steel bars. But FRP bars also have some drawbacks such as brittle failure and low ductile capacity which should be considered carefully in design. Considering their excellent linear-elastic behavior and high tensile strength, the combination of CFRP bars and dampers together to reinforce buildings may achieve multiple goals such as self-centering and large energy dissipation (damping), that is, CFRP bars help control the residual displacement and dampers can be used in some particular sites of buildings to absorb more earthquake energy. Then the first step is to study the validity and applicability of shear walls reinforced with CFRP bars. CFRP bars were used to replace steel bars as longitudinal reinforcement in this paper. In addition to studying the hysteretic property, stiffness, energy dissipation, the main purpose of this experiment is to investigate the effect of CFRP bars on displacement demand and residual deformation of shear walls. The strains of steel and CFRP bars at the boundary elements were measured by strain gauges. Crack patterns, residual cracks and residual displacements were recorded to evaluate the self-centering performance of shear walls reinforced with CFRP bars.

2. Methods and material

Three specimens were tested up to failure under quasi-static cyclic lateral loading. The first one (RCSW) was a conventional reinforced wall (as a reference specimen). The second (S-CFSW) was reinforced with steel bars in boundary elements and CFRP bars in the wall web as vertical reinforcement. The third (CFSW) was reinforced with CFRP bars totally in the vertical direction. They had same geometry and the aspect ratio was 2.33, which belong to medium-rise shear walls. The detailed information about shear wall specimens, material property and test setup are included in the following parts.

2.1. Design of shear wall specimens

Three specimens shared the same size in height, width and thickness, with h_w = 2800 mm, b_w = 1200 mm and t_w = 200 mm, respectively. The top of the wall was reinforced by steel bars in horizontal direction, and designed as a concealed beam to bear axial and lateral loads during the test. The dimensions of three walls are shown in Fig. 2. Fig. 3 illustrates the detailed reinforcement information. Three specimens were reinforced with two-layer grids of reinforcement bars. Each grid in the wall web was comprised of steel or CFRP bars in vertical direction (a vertical reinforcement ratio of 0.52%) and steel bars

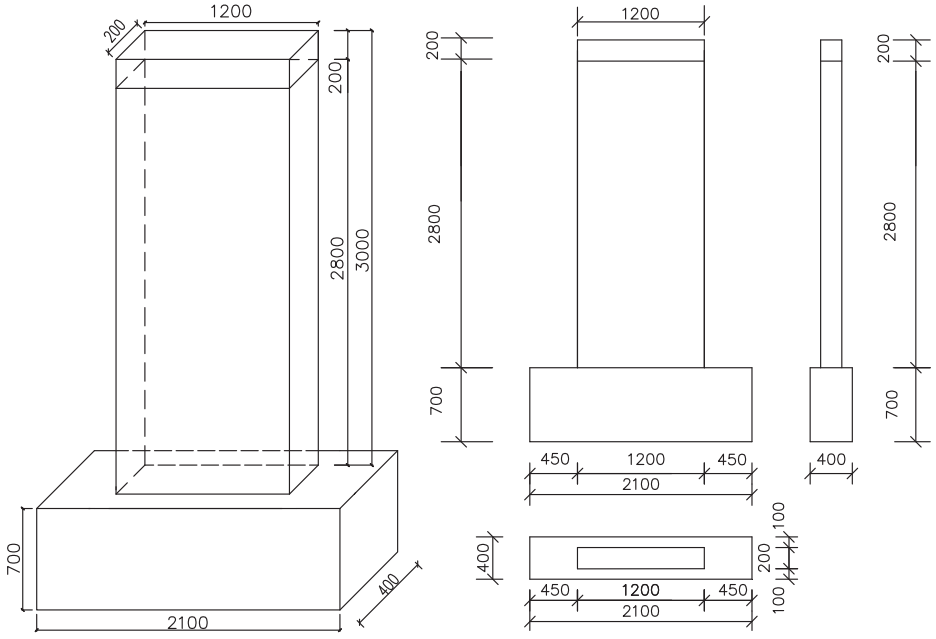

Fig. 2. Dimensions of specimens.

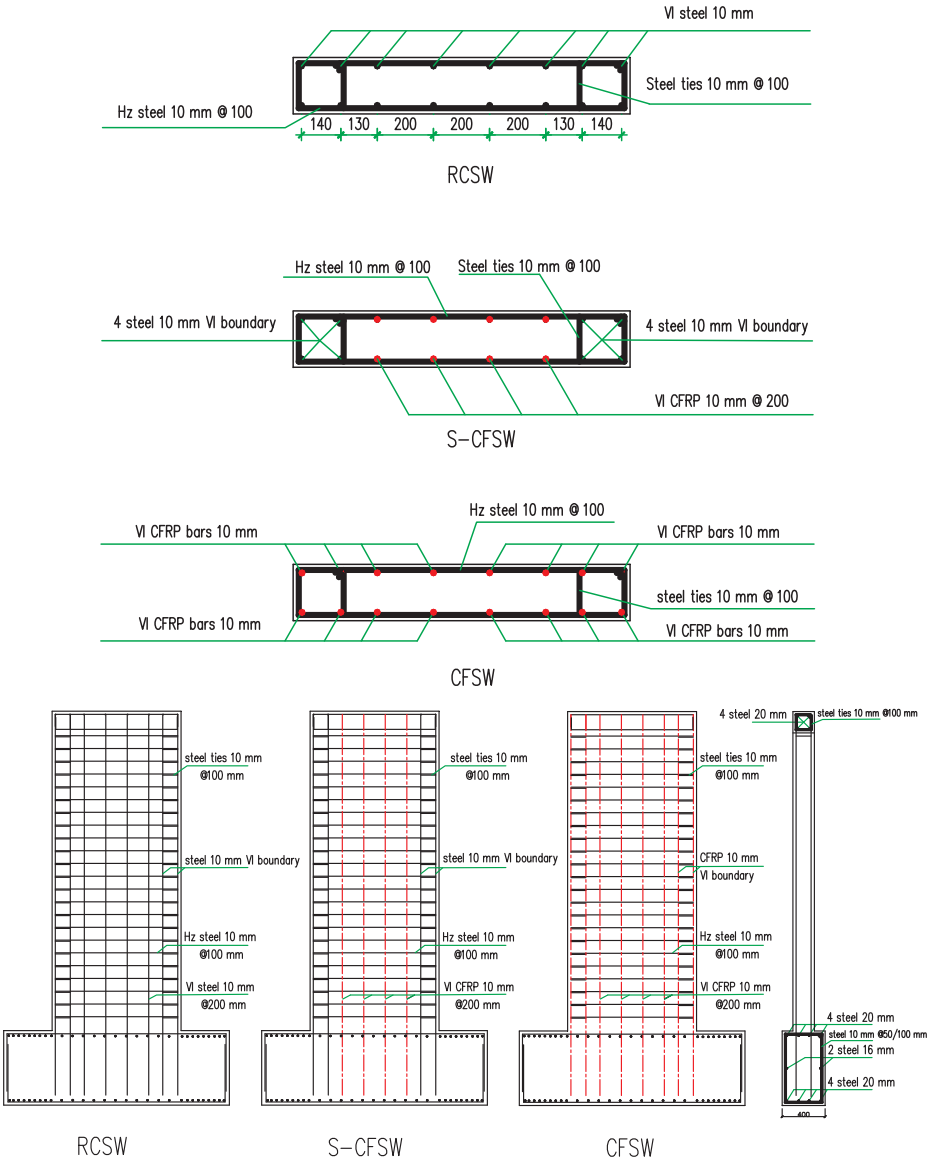

Fig. 3. Detailed information of reinforcement. *Notes*: VI denotes vertical reinforcement and Hz denotes horizontal reinforcement. For example, "Hz steel 10 mm @ 100 mm" means horizontal steel bars with 10 mm in diameter and a spacing of 100 mm.

(10 mm in diameter) with a spacing of 100 mm in horizontal direction (a horizontal reinforcement ratio of 0.79%). The seismic design code in China stipulates a minimum steel ratio of 0.25% in shear wall. And the minimum steel ratios of vertical and horizontal reinforcement by ACI 318 are 0.15% and 0.25%, respectively. Four steel bars (10 mm in diameter) were arranged in each boundary column (for RCSW and S-CFSW) with the same cross-section (200 mm × 200 mm). Likewise, four CFRP (10 mm in diameter) bars were placed in each boundary of CFSW. Steel stirrups (10 mm in diameter) were spaced at 100 mm in the boundary columns. All shear walls complied with the requirements of minimum reinforcement ratio and thickness of shear walls suggested by codes [20–22]. The reinforcement details are illustrated in Fig. 3.

2.2. Material properties

The shear wall specimens were constructed and tested in the lab of structural engineering. C45 commercial concrete which is widely used for main supporting members in construction was adopted. 12 concrete cubes (150 mm × 150 mm × 150 mm) and 9 concrete prismatic blocks (150 mm × 150 mm × 300 mm) were reserved in the same condition with shear wall specimens according to Chinese code [23]. Table 1 gives the tested values of concrete compressive strength, tensile strength and elastic modulus. The tensile strength of steel bars HRB400 was gained according to GB/T 228.1-2010. And the longitudinal tensile strengths of CFRP bars were collected through testing 5 specimens according to GB/T 26743-2011. Table 2 lists the mechanical properties of steel and CFRP bars.

Table 1
Mechanical properties of concrete.

f_{cu} (MPa)	f_c (MPa)	f_t (MPa)	E (MPa)
56.75	43.47	3.4	4.52×10^4

Notes: f_{cu} = cubic compressive strength of concrete; f_c = axial compressive strength; f_t = split-tensile strength; E = elastic modulus in compression.

2.3. Test setup and loading procedures

The test setup is illustrated in Fig. 4. Cyclic Lateral forces were imposed on specimens through an actuator fixed horizontally to the reaction wall. An axial load of 10% of its design compressive capacity

Table 2
Mechanical properties of steel bars and CFRP bars.

Material	D (mm)	f_y (MPa)	f_u (MPa)	ε_y or ε_{fu}	E (MPa)
HRB400	10	424	658	0.0019	2.24×10^5
CFRP bar	10	–	1102	0.0118	9.7×10^4

Notes: D = diameter of bars; f_y = yielding strength; f_u = tensile strength; ε_y = yielding strain of steel bars; ε_{fu} = ultimate tensile strain of CFRP bars; E = elastic modulus in tension.

(1080 kN) was induced on the top of the wall and remained constant throughout testing. The axial loads were provided by two synchronous hydraulic cylinders that could move horizontally and smoothly. The shear wall specimens were fixed on the heavy box-beam of the ground. Lateral displacements were recorded at the height of 600 mm, 1200 mm, 1700 mm, 2200 mm, and 2700 mm at two sides of the wall. An automatic data-acquisition system monitored by a computer was used to collect various data. Crack progression and width were marked and recorded throughout the loading. The force-displacement controlled method was adopted as shown in Fig. 5. At force-controlled stage, the lateral load was cycled only once and the increase of lateral force was 10 kN. Displacement-controlled method took over when steel yielding occurred. Considering the fact that there is no yielding strain in CFRP bars until failure, the yielding displacement of RCSW was used as the increase of displacement Δ for all specimens. This makes easy to compare their behaviors such as energy dissipation and residual displacement between them at the same displacement levels/cycles. Shear walls were cycled three times at each displacement level. When 85% of ultimate lateral strength occurred after strength degradation, loading should be terminated and the specimen was considered to be failure.

3. Experimental results and discussions

3.1. Lateral load-top displacement response

Hysteretic curves of three specimens are shown in Fig. 6. The curves of RCSW and S-CFSW were similar. And the longitudinal steel bars at boundary elements yielded when lateral drift rose up to 0.13% and 0.12% in RCSW and S-CFSW, respectively. Hysteretic loops of the traditional wall were plumper than those of S-CFSW at the same drift levels. In particular, CFSW had much more pinched hysteretic loops than the other walls.

Fig. 7 illustrates the envelop curves of the three walls. RCSW, S-CFSW and CFSW achieved similar lateral peak loads with 372.74 kN, 372.5 kN and 380.28 kN in the positive direction. And they reached peak loads at a lateral drift of 1.4%, 1.2% and 1.2%, respectively. Then their lateral forces fell to 85% of peak values at a drift ratio of 1.54%, 1.41% and 1.33%, at which specimens were considered to be failure. From yielding to peak load, permanent deformations were evidenced by plump loops of hysteresis curves in RCSW and S-CFSW, in comparison to pinched cycles of CFSW. Three specimens were subjected to flexure and shear forces. As lateral displacement increased, all the walls fell to failure finally, along with concrete cover spalling, crushing and then vertical reinforcement materials fractured at their boundaries. The reference specimen had the largest drift capacity. It also had larger lateral strength than the others at the same drift during the negative loading. When a lateral displacement was imposed on the wall, steel bars could bear more loads than CFRP material before steel yielded due to larger elastic modulus. This may be the reason why steel-reinforced wall had a lager reaction force than two others before 0.25% drift. Two factors may cause the non-symmetric response in S-CFSW and CFSW. One is concrete damage, the other is the bond slip between CFRP bars and concrete. When the displacement level increased, it would cause concrete damage first in the positive cycle. Considering that the bond between CFRP bars and concrete is not as good as that between steel and concrete, the bond slip between CFRP bars and concrete might also contribute to the non-symmetric response. Then during the following negative loading, the CFRP-reinforced shear wall would not perform as well as in the positive loading. Since RCSW had the largest drift capacity between them, this type of system would not be ideal now for regions with high seismic hazards where large displacement demands are expected. In the authors' view, the lower elastic modulus of CFRP bar (only 97 GPa used in this experiment) might limit its potential of high tensile strength. The advantage of CFRP bars started to develop after the steel yielded. CFRP bars with better bond conditions and further study are still needed to identify this feature.

3.2. Crack patterns and failure progression

The first crack emerged in CFSW when the lateral force reached 40 kN. For S-CFSW and RCSW, however, crack started to develop when loads reached 70 kN and 80 kN, respectively. As lateral force continued,

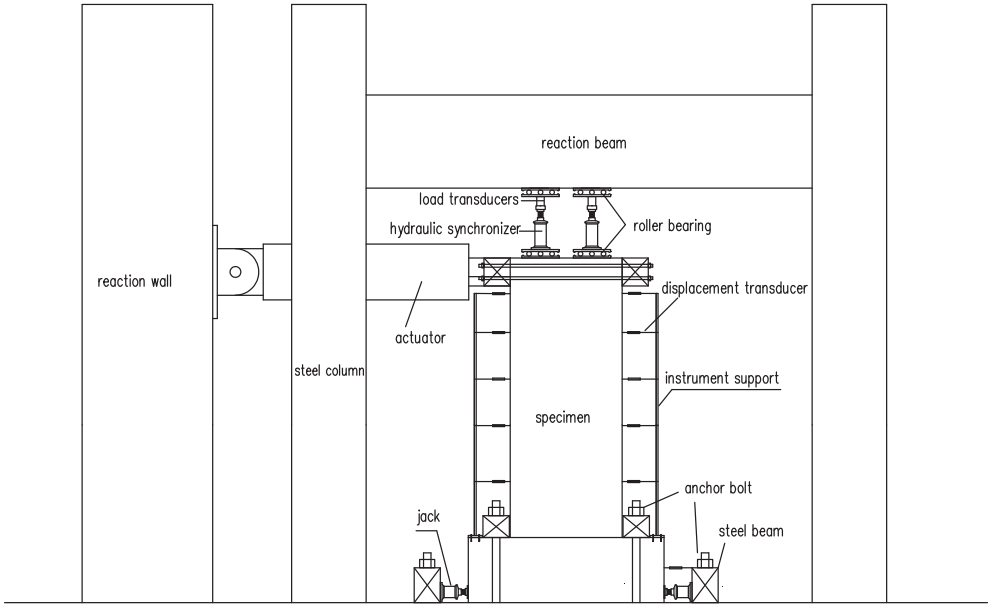

Fig. 4. Instrument and test setup.

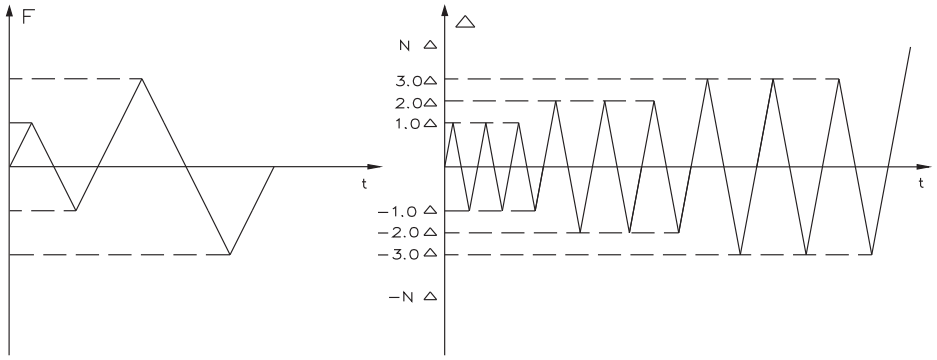

Fig. 5. Loading protocol.

more horizontal cracks began to form up. And the original cracks propagated more deeply, then followed by flexural-shear cracks. Figs. 7 and 8 illustrate crack patterns and crack process at different drifts. Cracks are numbered according to the sequence of emerging. RCSW evidenced smaller initial crack than the others when lateral drift was less than 0.27%. With loading increasing, RCSW experienced a wider crack as a result of steel yielding in boundary elements. However, more cracks were clearly found in CFRP-reinforced walls. Their cracks nearly doubled compared with cracks in RCSW. Besides, cracks were only distributed along 1/3 of RC wall, while cracks spread up to approximately a 2/3 of wall height in the two others. The fact indicates that CFRP bars reduced deformation concentration. More small and narrow cracks developed along the two latter walls. The steel bars in RCSW yielded at the bottom and remained large residual deformations. Then less but wider cracks remained. Although more narrow cracks may cause some discomfort for occupants, they are easier to be repaired than those larger ones. Overall, cracks were distributed more widely in CFSW and S-CFSW than in RCSW, which indicates the use of CFRP bars has promoted their crack spreads.

The difference of failure progressions between RCSW, S-CFSW and CFSW was that there was a sharp turn in envelop curves of RCSW and S-CFSW, while the envelop curve of CFRW was smoother until failure. The turning point occurred after yielding of steel bars at the boundary columns, as shown in Fig. 7. The CFRP-reinforced wall CFSW went on carrying loads without strength deterioration until concrete crushing on the compression side and the fracture of vertical CFRP bars on the

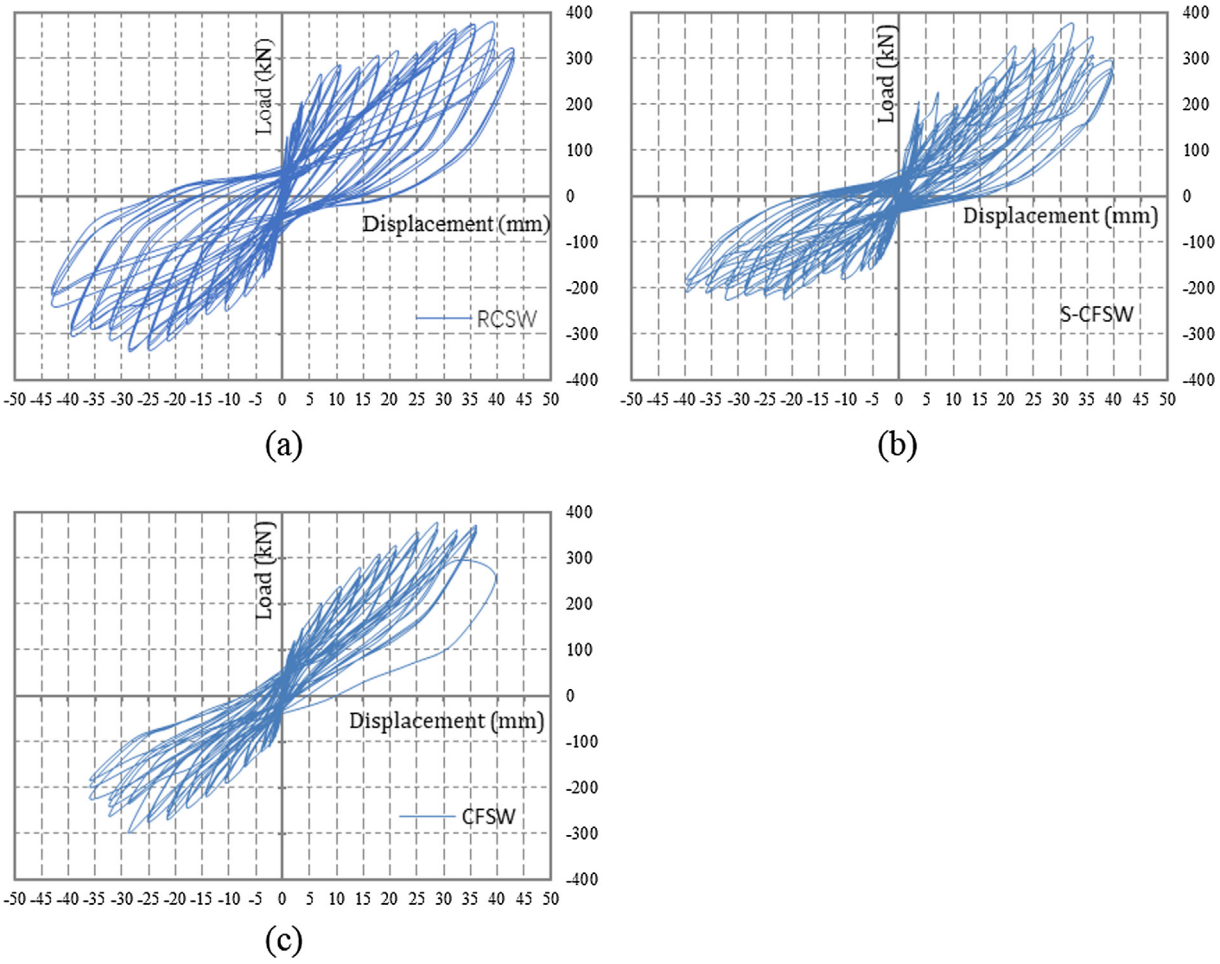

Fig. 6. Hysteretic loops of specimens: (a) hysteretic loops of RCSW; (b) hysteretic loops of S-CFSW; (c) hysteretic loops of CFSW.

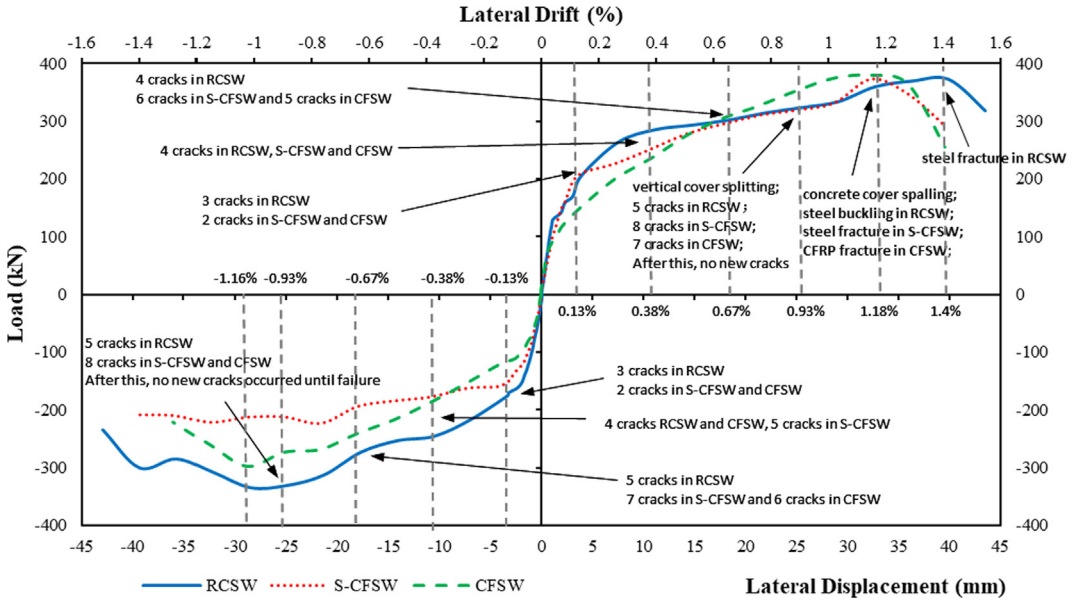

Fig. 7. Envelop curves of specimens.

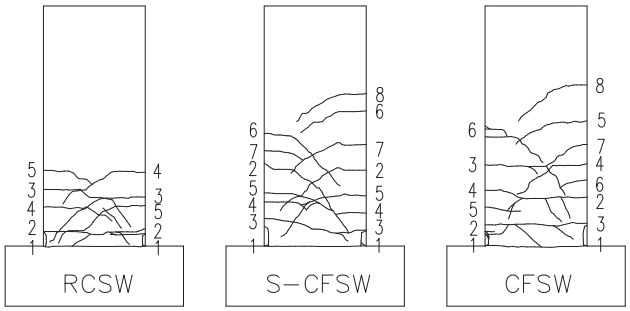

Fig. 8. Crack patterns of specimens.

tension side. By contrast, the reference wall RCSW experienced the buckling of steel bars and concrete cover crushing at the compression side of the wall. As displacement increased, concrete spalling and crushing along with longitudinal bars' buckling occurred at the compression side, associated with the fracture of vertical bars at tension side, as illustrated in Fig. 9. Then the lateral strength decreased sharply. The failure progression of S-CFSW was similar to RCSW. Although the displacement capacity and load capacity between the three walls were different, concrete cover spalling occurred when the lateral drift reached 1.2%. For S-CFSW and CFSW, steel bars and CFRP bars in the boundary elements fractured at this drift level. But the fracture of steel bars in RCSW happened when the drift reached 1.4%. CFSW had brittle failure, more cracks, and less displacement capacity compared to the reference.

3.3. Secant stiffness

Stiffnesses at various displacement levels were calculated and the secant stiffness versus lateral displacement curves are illustrated in Fig. 10. The slope of hysteretic curves decreased at 0.13% drift, reflecting the stiffness degradation of shear walls. Stiffness deterioration took place in all specimens as drift levels increased. Despite a similar pattern of stiffness degradation, some discrepancies could also be observed among them. While RCSW and S-CFSW experienced higher stiffness up to the lateral drift of 0.56%, after that, CFSW had similar or even a little higher post-yield stiffness. As discussed in Section 3.1, CFRP bars with larger tensile stiffness may make CFRP-reinforced shear wall have larger lateral load capacity and post-yield stiffness than the steel-reinforced wall. In the authors' view, adequate post-yield stiffness is important for buildings to avoid collapse during aftershocks. Higher post-yield stiffness can make structures work better in areas where severe earthquakes happen frequently.

3.4. Energy dissipation and pinching

There is a widespread consensus among researchers and scholars that the energy dissipation ability is an important parameter in evaluating seismic performance of structures, in addition to ductile capacity [2–5,24]. The energy absorbed by shear walls could be estimated by calculating the area of hysteretic loops. Fig. 11 shows the accumulated energy consumed versus numbers of half cycles. It can be seen that before 18 half cycles (a lateral drift of 1/375), there was no significant difference in energy dissipated by RCSW, S-CFSW and CFSW. Little residual deformations were left when the load was released. Accumulated energy, however, increased rapidly after 18 half cycles, especially for RCSW. The total energy absorbed by RCSW was 72773.2 kN mm at 48 half cycles (a lateral drift of 1.0%), in comparison to only 46259.9 kN mm in S-CFSW and 34804.2 kN mm in CFSW at the same drift. Then it reached up to 128,284 kN mm at the drift of 1.2% (corresponding to the peak load), compared with 75,778 kN mm and 54,664 kN mm at the same drift for S-CFSW and CFSW. The energy absorbed by RCSW doubled the amount dissipated by CFSW, which demonstrates shear walls reinforced by steel bars could absorb much more energy than the walls reinforced with CFRP bars. This may be attributed to the excellent plastic behavior of steel bars. Through plastic deformation more energy could be absorbed, while CFRP bars remained in elastic all the time until failure.

From a traditional point of view, adequate drift capacity and large energy dissipation are considered two desirable and long-cherished design goals for shear walls [3]. For a long time, hysteretic pinching was recognized as an undesirable characteristic by engineers and researchers, and they thought it is adverse for these structures to withstand seismic activities. However, recent studies [15,25,26] conveyed a different view towards hysteretic pinching that hysteretic pinching without stiffness deterioration will not lead to undesirable response directly. Based on some SDOF studies, Krawinkler and Seneviratna [27] has concluded that pinching does not have a significant effect on the inelastic displacement demand for SDOF except for very short period systems. In order to investigate the dynamic impact in the global

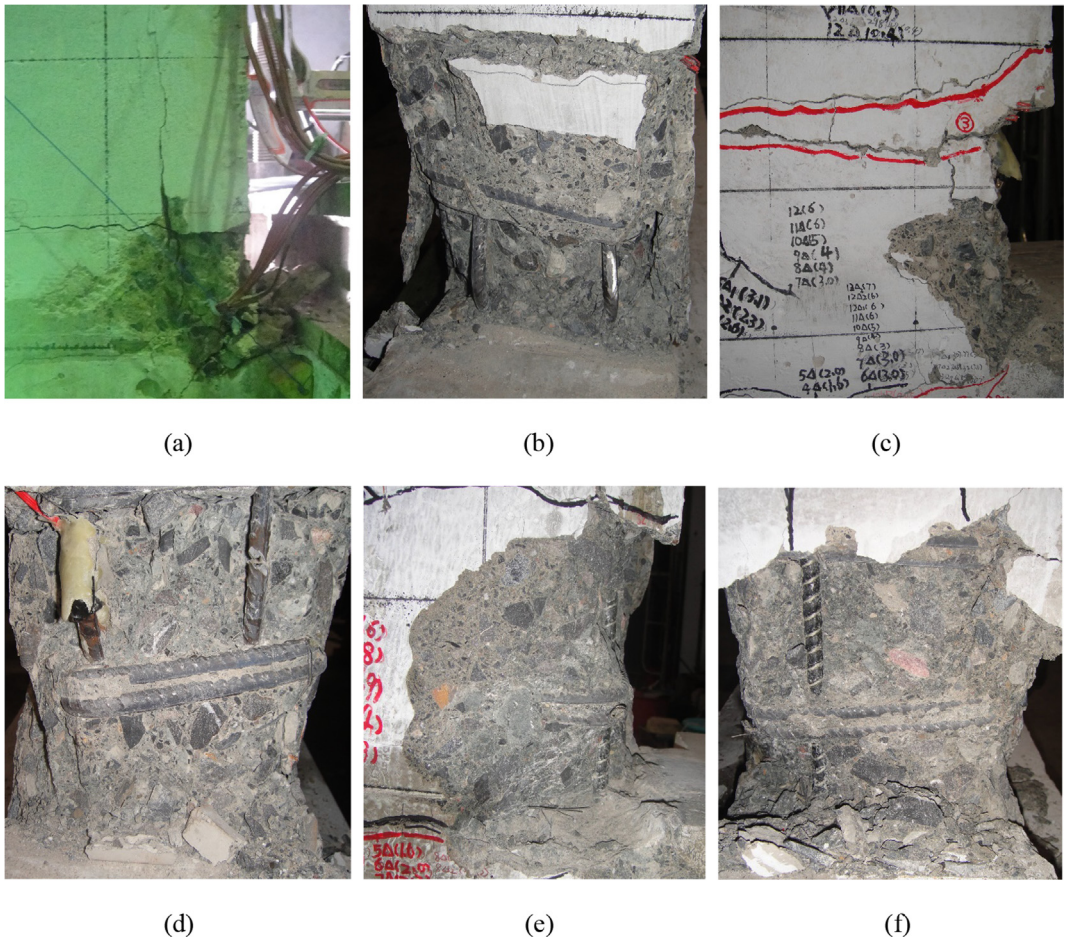

Fig. 9. Failure Progression of Specimens: (a) concrete cover splitting; (b) the bucking of vertical steel bars; (c) concrete cover spalling; (d) the fracture of vertical steel bars; (e) concrete crushing; (f) the fracture of vertical CFRP bar.

response of shear walls with varying pinching characteristics, a single degree of freedom system model and a bilinear hysteretic model (as shown in Fig. 12) have been adopted to evaluate the displacement responses under a few ground motions. Several earthquake motions (El Centro 1940, Kobe-CHY 1995, Taft 1952 in two directions) are selected to perform the SDOF time-history analysis. A matlab program is used to calculate the dynamic response by applying Newmark's linear acceleration method. All parameters of two SDOF examples (RC wall and CF

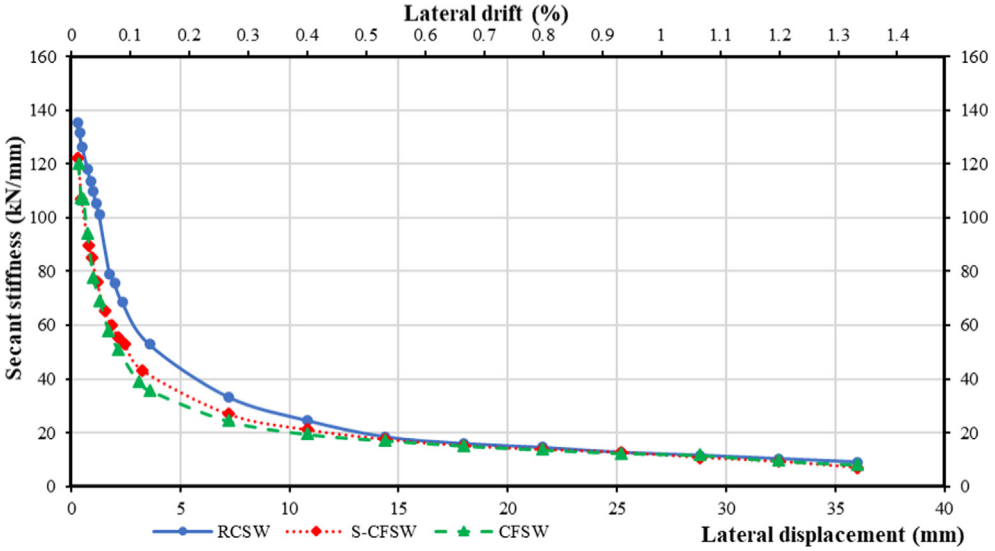

Fig. 10. Secant stiffness – lateral displacement curves. Notes: The secant stiffness is defined by $K = \frac{|F_+| + |F_-|}{|D_+| + |D_-|}$; F_+ = the maximum lateral force during the positive cycles; F_- = the maximum lateral force during the negative cycles; D_+ = the lateral displacement corresponding to F_+; D_- = the lateral displacement corresponding to F_-.

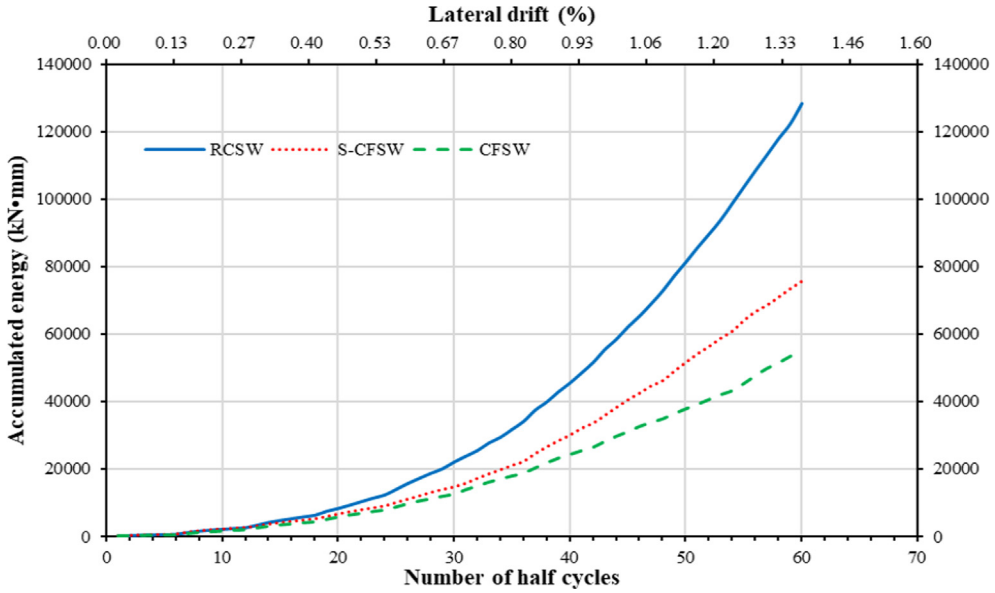

Fig. 11. Accumulated energy curves.

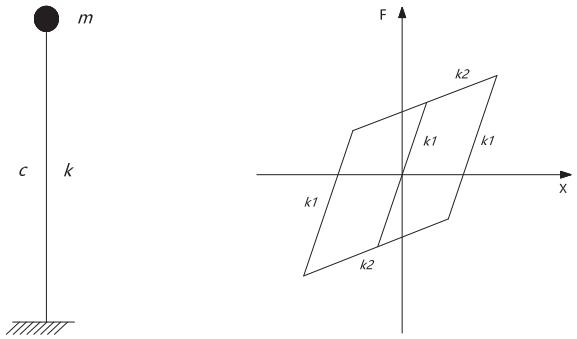

(a) Single degree of freedom system (b) Bilinear hysteretic model

Fig. 12. Simplified SDOF model and time-history analysis model adopted.

wall) are obtained from the data of RCSW and CFSW in this experiment (in this case, the given mass is 108,000 kg, for RC wall, K1 = 80,000,000 N/m, r = K2/K1 = 0.05, c = 100,000 N s/m; for CF wall, K1 = 70000000 N/m, r = K2/K1 = 0.11, c = 100000 N s/m). The time-history analysis results are shown in Table 3. From the results, it can be seen that, for SDOF system, pinching does not have a consistent effect on the displacement demand under different earthquake motions. According to the maximum displacement demands (measured by maximum absolute values in positive and negative directions) from the analysis results in Table 3, it might be hard to conclude that pinching will always amplify the displacement demands of structures during different ground motions. It is not very clear about the actual effect of pinching on the displacement demand of MDOF systems, and further research is still needed.

3.5. Crack width and residual deformation

Crack width and residual displacement were recorded in this paper. The maximum values of crack width at different lateral drifts are shown in Fig. 13. Fig. 14 shows the residual displacements at various lateral displacements. Several findings can be seen from the following figures. The maximum crack of RCSW, S-CFSW and CFSW was 1.08 mm, 1 mm and 1.06 mm, respectively at 0.25% drift. However, cracks in RCSW and S-CFSW grew larger rapidly with increased displacements, and were up to 4 mm and 3 mm at the drifts of 0.9%, then reached 4.4 mm and 4 mm at 1.06% drift. By contrast, the maximum crack in CFSW remained less than 2 mm until 0.9% drift, and reached only 2.4 mm at 1.06% drift. This indicates that the crack progression of steel-reinforced shear walls RCSW mainly concentrated on the bottom of the wall where steel bar yielded. This can also be verified by their crack patterns in Fig. 8.

The lateral residual deformations of all specimens remained small at 0.25% drift. Before this drift level, the maximum residual deformation of RCSW and S-CFSW were 1.0 mm, while there was no residual deformation in CFSW. The residual deformation in RCSW increased sharply up to 8 mm, 10 mm, 13 mm when the lateral drift reached 0.89%, 1.0%, and 1.28%, respectively. Despite of a flat growth of lateral drift from 0.4% to 0.77%, S-CFSW showed a similar trend as RCSW, and its residual deformation rose up to 4 mm, 4.9 mm and 9.1 mm at lateral drifts of 0.89%, 1.0% and 1.28%. By contrast, there was no sharp growth of residual deformations for CFSW. Its residual deformation was less than 2 mm until failure. The results indicate that CFRP bars can provide remarkable centering performance compared to steel bars. The allowable inter-story drifts for shear wall structures are required to be less than 1/120 (0.83% lateral drift) by Chinese code GB50011-2010, corresponding to a lateral displacement of 6Δ in this paper. And at this level, the residual deformations of RCSW, S-CFSW and CFSW were 5.8 mm, 2.4 mm and 1.5 mm, respectively. Fig. 7 shows that all specimens experienced a rising lateral strength until 8Δ (a lateral drift of

Table 3
Maximum displacement demands under different earthquake motions.

Maximum displacement demand	El Centro (N-S) (W-E)		Kobe-CHY (N-S) (W-E)		Taft-Lincoln Sch (N-S) (W-E)	
RC wall (reference)	10.4 mm	10.1 mm	4.2 mm	4.8 mm	9.1 mm	−9.3 mm
CF wall	−13.8 mm	14.6 mm	3.8 mm	−3.7 mm	7.8 mm	−11.1 mm
Displacement demand ratio	−1.33	1.45	0.90	−0.77	0.86	1.19

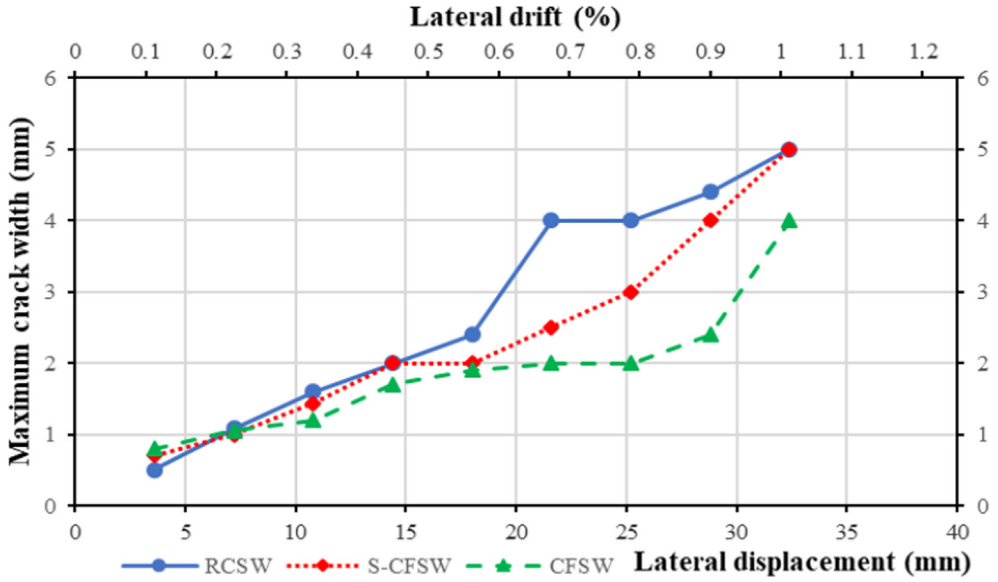

Fig. 13. Maximum crack width – lateral displacement.

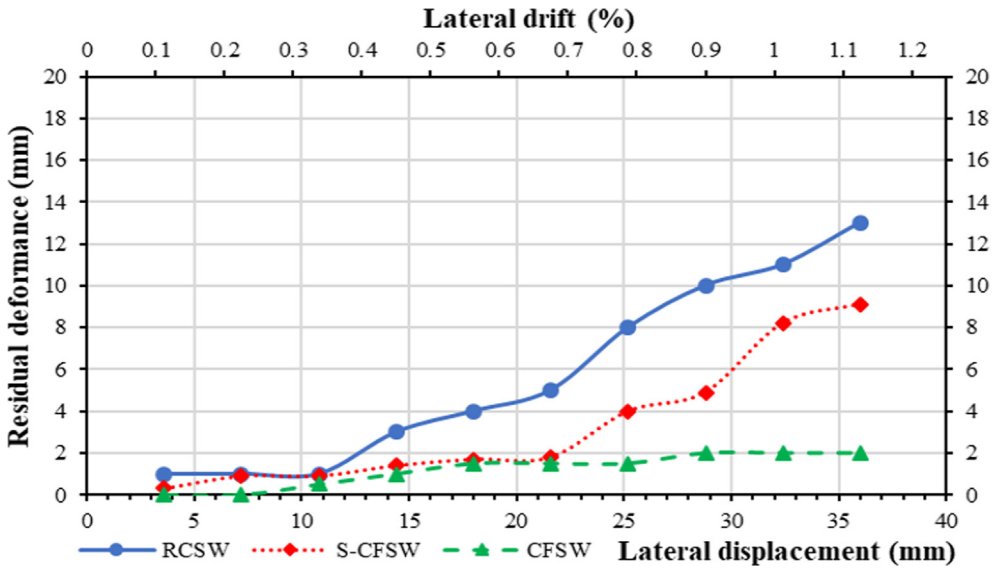

Fig. 14. Residual deformation at various lateral displacements.

1.0%). Three shear walls had enough lateral drift capacities and the data show it was possible for CFRP bars to be used in reinforcing shear walls in the future. Hence, it could be seen that well-designed wall reinforced with CFRP bars could meet the deformation requirements by codes, and they will have less residual deformation after cyclic loading than RC walls.

Hysteretic loops reflect different levels of energy dissipation and self-recentering behavior. A pinched loop represents less energy dissipation, but it also leaves less residual displacement. The results demonstrate that using CFRP bars can help control the maximum crack, increase crack spread, reduce deformation concentration and improve self-centering behavior. The ability of recovering and reclosing cracks after experiencing large drifts could be recognized as an excellent advantage of using CFRP bars.

4. Conclusion

This paper aimed to verify the feasibility of using CFRP bars to reinforce shear walls, and to identify their effect on self-centering behavior, in addition to achieving acceptable displacement capacity and stiffness to resist lateral forces. Three walls were tested up to failure under quasi-static cyclic loading. CFRP bars were used as the longitudinal reinforcement material in two walls, one traditional RC wall was designed as a reference. Some valuable findings could be concluded as follows:

- The crack progressions of three shear walls were similar. They were dominated by flexure at first, then controlled by the combination of flexure and shear forces under larger drifts until failure. But CFSW had more cracks and a wider spread of cracks than RCSW.
- The CFRP-reinforced concrete shear wall achieved acceptable capacity, post-yield stiffness and less drift capacity compared with the reference wall. But the displacement capacity can still meet the requirement by code such as GB 50011-2010.
- Pinched hysteretic loops of CFSW indicate that the CFRP-reinforced shear wall has less residual deformation and excellent self-centering behavior, while plump hysteretic loops of RCSW show that the conventional steel-reinforced shear wall can absorb more energy.

- The use of CFRP bars in vertical direction made CFRP-reinforced wall have a wider spread of cracks, less displacement capacity and brittle failure in comparison to RC shear wall. However, the residual deformation of CFSW decreased by 81.3% and 84.7% at the lateral level of 0.89% and 1.28% compared with RCSW. Besides, its maximum crack width decreased by 50% and 45.5% at a lateral drift of 0.9% and 1.0%, respectively.
- Despite these interesting findings, further research is still needed before application and the effect of FRP bars on the energy dissipation and cracks of shear wall should be specially considered in design.

Acknowledgment

This research was supported by the National Key R&D Program of China [2016YFE0125600] and the Program for Changjiang Scholars & Innovative Research Team of Education Ministry of China [IRT_16R67]. The authors are also grateful to the support from PEER Ground Motion Database.

References

[1] Ahmed N, Mohamed AR. Strength and drift capacity of GFRP-reinforced concrete shear walls. Sherbrook: Scholars' Press; 2014.
[2] Mohamed N, Farghaly AS, Benmokrane B, Neale KW. Flexure and shear deformation of GFRP-reinforced shear walls. J Compos Constr 2014;18(2):785–93.
[3] Mohamed N, Farghaly AS, Benmokrane B, Neale KW. Evaluation of GFRP-reinforced shear walls. Canadian society for civil engineering 2013 general conference, Montréal, Québec, Canada. 2013. p. 1–10.
[4] Mohamed N, Sabry Farghaly A, Benmokrane B, Neale KW. Experimental investigation of concrete shear walls reinforced with glass fiber-reinforced bars under lateral cyclic loading. J Compos Constr 2014;18:1–10.
[5] Mohamed N, Ahmed SF, Benmokrane B. Evaluation of a shear wall reinforced with glass FRP bars subjected to lateral cyclic loading. 3rd Asia-pacific conference on FRP in structures, Sapporo, Japan. 2012. p. 1–10.
[6] Cardenas AE, Hanson JM, Corley WG, Hognestad E. Design provisions for shear walls. ACI J 1973;70(3):221–30.
[7] Wyllie LA, Abrahamson N, Bolt B, Castro G, Durkin ME. The chile earthquake of March 3, 1985- performance of structures. Earthq Spectra 1986;2(2):93–371.
[8] Fintel M. Performance of buildings with shear walls in earthquakes of the last thirty years. PCI J 1995;40(3):62–80.
[9] Zinov'ev PA, Smerdov AA, Kulish GG. Experimental investigation of elastodissipative characteristics of carbon-fiber-reinforced plastics. Mech Compos Mater 2003;39(5):393–8.
[10] Liang XW, Ma KZ, Li FF, Deng MK, Zhang XH. Experimental study on seismic behavior of SHSC structural walls. J Build Struct 2011;32(6):68–75. [in Chinese].
[11] Guo LH, Ma XB, Zhang SM. Experimental research on steel plate shear wall with slits. Eng Mech 2012;29(3):133–42. [in Chinese].
[12] Li B, Li HN. Research on quasi-static test of reinforced concrete shear walls with different shear-span ratio. Ind Constr 2010;40(9):32–6. [in Chinese].
[13] CSG. Analysis on seismic damage of buildings in the Wenchuan earthquake. J Build Struct 2008;29:1–9. [in Chinese].
[14] Sun YP, Zhao SC, Zhao H. Seismic behavior and evaluation of sustainable and resilient concrete columns. China Civ Eng J 2013;46(5):105–10. [in Chinese].
[15] Sun YP, Takeuchi T, Funato Y. Earthquake-resisting properties and evaluation of high performance concrete columns with low residual deformation. 15th world conference on earthquake engineering, Lisbon, Portugal. 2012. p. 1–10.
[16] Zhao J, Zhao Q, Dang JT, Zeng LX. Experimental study of deformation behavior of shear wall reinforced with CFRP bars and steel bars. Ind Constr 2017;47(1):163–7. [in Chinese].
[17] Cai ZK, Wang D, Wang Z. Full-scale seismic testing of concrete building columns reinforced with both steel and CFRP bars. Compos Struct 2017;178:195–209.
[18] Ghazizadeh S, Cruz-Noguez CA, Talaei F. Analytical model for hybrid FRP-steel reinforced shear walls. Eng Struct 2018;156:556–66.
[19] Ghazizadeh S, Cruz-noguez CA. Damage-resistant reinforced concrete low-rise walls with hybrid GFRP-steel reinforcement and steel fibers. J Compos Constr 2018;22:1–12.
[20] ACI. Building code requirements for structural concrete and commentary. ACI 318-14, Farmington Hills, MI; 2014.
[21] CABR. Code for design of concrete structures. GB 50010-2010, Beijing; 2010. [in Chinese].
[22] CABR. Code for seismic design of buildings. GB 50011-2010, Beijing; 2010. [in Chinese].
[23] CABR. Standard methods for testing concrete structures. GB/T 50152-2012, Beijing; 2012. [in Chinese].
[24] Lu XZ, Ye LP, Miu ZW, Pan P. Elasto-plastic analysis of buildings against earthquake. Beijing: China Archit Build Press; 2011. [in Chinese].
[25] Huang Z, Foutch DA. Effect of hysteresis type on drift limit for global collapse of moment frame structures under seismic loads. J Earthq Eng 2009;13:939–64.
[26] Sharbatdar MK, Saatciogu M. Seismic design of FRP reinforced concrete structures. Asian J. Applied Sci 2009;2(3):211–22.
[27] Krawinkler H, Seneviratna GDPK. Pros and cons of a pushover analysis of seismic performance evaluation. Eng Struct 1998;20(4–6):452–64.